

Accuracy of Earth's Thermospheric Neutral Density Models

Frank A. Marcos¹
*Air Force Research Laboratory
Hanscom AFB, MA 01731-3010*

Bruce R. Bowman²
*Air Force Space Command
Colorado Springs, CO*

and

Robert E. Sheehan³
Boston College, Chestnut Hill, MA

[Abstract] Atmospheric drag remains the dominant uncertainty for low altitude satellite precision orbit determination. Empirical models are used to estimate satellite drag. Model accuracies have shown little improvement in the past 35 years. A new Jacchia-Bowman 2006 (JB2006) empirical model has been developed as part of the Air Force Space Command's High Accuracy Satellite Drag Model (HASDM) program. Significant new model features of JB2006 are solar indices based on satellite EUV and FUV sensors and an improved semiannual variation. This new model is compared to historic models vs altitude, latitude, local time, day of year and solar and geomagnetic conditions. Data are from a unique high-accuracy set of thermospheric neutral densities with one-day resolution, obtained from tracking of 38 satellites. The evaluation is carried out for the period 1997 through 2004, when the specific solar indices for JB2006 were available. The results provide improved understanding of quantitative relations between current solar inputs and the response of the thermosphere. New formulations incorporated into the JB2006 lead to a capability to more accurately specify thermospheric density.

I. Introduction

Aerodynamic drag continues to be the largest uncertainty in determining orbits of satellites operating in earth's upper atmosphere below about 600 km. Critical precision orbit determination and tracking operations include collision avoidance warnings for the International Space Station, satellite lifetime estimates, laser communication and reentry prediction. Errors in neutral density are the major source of drag errors. Orbital drag accelerations (a_D) for a satellite in the earth's atmosphere are related to neutral density by:

¹ Physicist, Space Vehicles Directorate, AFRL/VSBXT, 29 Randolph Road, Hanscom AFB, MA, 01731-3010, Member.

² Research Scientist, Space Analysis, AFSPC/A9AC, Atrium II, Suite 212, 1150 Academy Park Loop, Colorado Springs, CO 80910, Senior Member.

³ Research Physicist, Institute for Scientific Research, 140 Commonwealth Avenue, St. Clement's Hall 410, Chestnut Hill, MA 02467-3862.

This paper is declared a work of the US Government and is not subject to copyright protection in the US DOD Distribution A. Approved for public release; distribution unlimited.

$$a_D = -1/2 (C_D A/M) \rho V^2 \quad (1)$$

where ρ is the atmospheric total mass density and A , M , C_D and V are the satellite's area, mass, drag coefficient and velocity respectively.

The science and engineering communities utilize empirical models for satellite drag analyses. The major neutral density variations in the thermosphere: diurnal, seasonal, semiannual, solar activity and geomagnetic activity were first incorporated into the Jacchia 1964¹ (J64) model, laying the foundation for models still used today. The model is built on analytical height profiles of the temperature, which depend on latitude, local time, day of year, solar activity index $F_{10.7}$ and geomagnetic activity index (K_p or a_p). These dependencies are represented by simple analytic functions. The solar flux term was represented by two components, a daily value and a time-averaged value. These indices continued to be used in all empirical models. Height profiles of the major constituents are calculated as a function of exospheric temperature assuming diffusive equilibrium and fixed boundary conditions at 120 km. An exponential form for the temperature profile that was closely approximated by theoretical temperature profiles allowed the hydrostatic equation to be explicitly integrated to provide density as a function of altitude. The model inputs are position, time and geophysical indices for solar and auroral heating. Outputs are temperature, composition and density. While a semiannual variation was observed to vary from year to year, the mechanism was unknown. Therefore this variation was, and has continued to be, represented by a climatological average. The Jacchia 1970² (J70) model, based on additional drag data (~16 satellites in the 1960's), incorporated refined relationships between solar drivers and density, improved the semiannual variation climatology and moved the lower boundary to 90 km, using constant temperature and constituent densities. This model continues to be the basis for operational density models at Air Force Space Command. The model was slightly revised³ in 1971 for inclusion into the CIRA (COSPAR International Reference Atmosphere) 1972 model⁴. A final version, featuring new local time and geomagnetic activity variations, was published in 1977⁵.

The NASA MET⁶ (Marshall Engineering Thermosphere) was developed by the NASA Marshall Space Flight Center. The model is essentially J70, but with a 162 day averaged solar flux compared to the 81 day average of J70. It provides total mass density, temperature and composition, and is used operationally for satellite lifetime estimates, orbit insertion, orbit determination and tracking, attitude dynamics and reentry prediction.

The Drag Temperature Model (DTM) combined satellite drag, accelerometer, and satellite composition and temperature data to construct a three-dimensional thermospheric model^{7,8} of temperature, density and composition based on diffusive equilibrium. An iterative procedure was used to obtain representation of the three major constituents N_2 , O and He in terms of spherical harmonics at 120 km altitude. Using a thermopause temperature model and an analytical temperature profile, concentrations for the major atmospheric constituents at a given altitude are computed as a function of solar and geophysical parameters. The current version of DTM⁹ has temperature and gradient at 120 km in agreement with ISR and satellite borne interferometer data and AE data, and capability to use the MgII index in place of F_{10} . Our version of the model did not have this provision. Therefore the model was eventuated using F_{10} .

The Mass Spectrometer and Incoherent Scatter (MSIS) series of models¹⁰⁻¹⁴ developed between 1977 and 1990, are used extensively by the scientific community for their superior description of neutral composition. The models utilized atmospheric composition data from instrumented satellites and temperatures from ground-based radars. The initial MSIS 1977 model¹⁰ was based on the Jacchia temperature profile framework, but the density at 120 km varied with local time and other geophysical parameters to fit the measurements. Exospheric temperature and density variations were represented by spherical harmonics resulting in requiring fewer parameters for a given level of accuracy. Subsequent versions of the model include the longitude variations¹¹, a refined geomagnetic storm effect¹², improved high latitude, high solar flux data¹³ and a boundary lowered to sea level¹⁴. The NRLMSISE-00¹⁵ model of atmospheric composition, temperature, and total mass density from ground to exobase includes the following: (1) drag data based on orbit determination, (2) more recent accelerometer data sets, (3) new temperature data derived from Millstone Hill and Arecibo incoherent scatter radar observations, and (4) observations of $[O_2]$ by the Solar Maximum Mission (SMM), based on solar ultraviolet occultation. A new species, "anomalous oxygen," primarily for drag estimation, allows for appreciable O^+ and hot atomic oxygen contributions to the total mass density at high altitudes.

The new Jacchia-Bowman (JB2006)¹⁶ model is based on the Jacchia model heritage. The major differences are in the solar flux input and in the semiannual formulation. A corrected local time variation is also implemented. JB2006 inserts the improved J70 temperature formulations into the CIRA 1972 model to permit integrating the diffusion equation at every point rather than relying on look-up tables. Solar indices are based on three components:¹⁷ S_{10} , based on data from SOHO EUV sensors, Mg_{10} based on FUV MgII sensors and a contribution from F_{10} . The semiannual variation is variable with height and time, and dependent on solar flux¹⁸. The density data used to

develop the new model equations are very accurate daily values obtained from drag analysis of numerous satellites with perigee altitudes of 175 km to 1100 km throughout the period 1978 through 2004. Approximately 120,000 daily temperature values were computed using a special energy dissipation rate (EDR) method¹⁹, where radar and optical observations are fit with special orbit perturbations. JB2006 is currently applicable for the period 1997 through 2004, when the required solar indices are available.

An evaluation of several versions of the empirical models available prior to JB2006, using accelerometer density measurements near 250 km, showed that both the Jacchia and MSIS types of models actually do remarkably well in describing the thermospheric variability. However, they all had similar one-sigma errors of about 15% for a given data set²⁰. Limitations of solar flux and semiannual formulations were found to be significant limiting factors²¹. We directly compare the accuracy of the JB2006 with the J70, NRLMSIS, NASA MET and DTM models over the 1997-2004 period. This comprehensive evaluation is mainly based on a unique high-accuracy, one-day resolution thermospheric neutral density database derived from tracking of 38 satellites having perigees between 200 and 1100 km.

A detailed description of the database used for evaluation is given in Section II. Section III provides comparisons of orbital drag to the models vs altitude, latitude, local time day of year and solar and geomagnetic conditions to quantify the various model accuracies, strengths and weaknesses. This evaluation is extended to the region above 600 km, to 1100 km, using densities obtained from tracking of six satellites. Results are summarized in Section IV.

II. Database

Our primary objective is to evaluate density model performance in the 200-600 km altitude region where satellite drag is the dominant source of tracking errors. A secondary objective is to extend the evaluation to about 1100 km altitude. We have an extensive representative set of data capable of evaluating models in the region of maximum importance, with densities from 38 satellites for the period from 1997 through 2004. The data were derived using the method of Bowman et al¹⁹ to obtain densities with one-day temporal resolution for the first time from satellite tracking observations. The density errors are estimated to be less than 5%. Fig. 1 provides satellite number, name, shape ballistic coefficient, inclination, perigee and apogee height in year 2000, and total period for which data are available. Approximately 75,000 daily density values were obtained for the period 1997-2004 throughout the altitude region from about 200-600 km. These are the first 32 satellites listed. Satellite perigees typically varied by about 20 km during the period studied. A second set of data from six satellites (the last six on the list in Fig.1) are utilized to examine density errors in the region from 650 km to 1100 km. These satellites were in nearly circular, polar orbits and are discussed in Section III-H below.

Each daily derived density value is assigned to a specific altitude, latitude and local time. Because the data are averaged, the drag is effective over a range of altitudes and latitudes. The fractional drag vs latitude was examined for a variety of satellite eccentricities and inclinations for a range of solar flux values. We show typical results for a 90-degree inclination satellite with perigee at 350 km and average solar flux conditions in Fig. 2. The simulation starts with the satellite at apogee over the equator. It moves toward the south pole, accumulating relatively little drag and continues down toward perigee at the equator at which point it has accumulated half of its total orbital drag. The other half of the drag comes from motion up to apogee via northern latitudes. For a 350 x 1000 km orbit, 80% of the drag occurs between +/- 33 degrees and 90% occurs between +/- 43 degrees. With a 350 x 5000 km orbit, the 80 and 90% altitude ranges reduce to +/- 16 and +/- 20 degrees respectively. The choice of elliptical orbits therefore permits characterizing density variability vs latitude and local time as well as solar and geomagnetic conditions.

To determine the optimum performance of JB2006 we perform our statistical analyses only on those days for which JB2006 are available, as indicated in Fig. 3. Zeroes indicate loss of data for a given day. There is a pronounced gap in the data for the period 2 May 1998 to 22 April 1999 when SOHO was not operating. In addition to these 331 days, there are an additional 91 days when data are not available. Overall the appropriate JB2006 solar data were available on 2499 of the 2921 days between 1 Jan 1997 and 31 Dec 2004. This chart also shows F10.7 and daily average ap values. Our evaluations are applicable to conditions representative of a solar cycle.

An example of the extensive data coverage is shown in Fig. 4. The number of points is displayed in latitude-solar flux, latitude-geomagnetic activity, latitude-local time, latitude-day of year coordinates. These plots demonstrate the adequacy of the dataset to evaluate models as a function of latitude, day of year, local time solar flux and geomagnetic activity as well as altitude. The latitude bins are 5 degrees in each case. It can be seen that there are hundreds of points per 10 solar flux unit (sfu) bins from solar minimum to beyond 200 flux units. The day of year bins are at a high resolution of 5 days, resulting in about 2600 bins, resulting in a rough average of about 30 points per bin. Similarly, local time bin sizes are 0.5 hours. An average bin contains about 50 points.

III. Results and Discussion

The quantity statistically analyzed is the ratio, R , between measured density and model density. The main focus is on analyzing the mean ratios

$$\bar{R} = \sum_{i=1}^N \frac{R_i}{N} \quad (2)$$

where R_i is the ratio of the i th density measurement to the model and N is the total number of data points, and the standard deviation is given by

$$S = \left[\sum_{i=1}^N \frac{(R_i - \bar{R})^2}{N-1} \right]^{1/2} \quad (3)$$

For a normal distribution about 68.3% of the data fall in the interval $\bar{R} \pm$ one sigma values given in this report.

Sections A to G deal with data in the prime region of interest for satellite drag, approximately 200-600 km. Section H emphasizes orbital drag data from six satellites in the altitude region of approximately 650-1100 km.

A. Frequency Distributions

The initial evaluation was to directly compare frequency distributions (data to model ratios vs number of cases) for the JB2006, J70, DTM, NRLMSIS and MET models using all data from 32 satellites in the altitude region 200-600 km. Density ratios were plotted in 0.01 model ratio step sizes and a Gaussian curve was added for each model by finding the equation of a normal distribution with the same mean and standard deviation as the given data. Fig. 5a shows results for JB2006, J70, DTM and NRLMSIS. MET are not shown, but the results are essentially identical to those of J70. The statistics are for all available solar and geomagnetic conditions. For all models the mean is near 1.0. JB2006 mean ratios are slightly lower than those of the other models, by 3.8%, 2.0% and 1.6% relative to J70, NRLMSIS and DTM respectively. The most striking result is that the standard deviation for JB2006 (0.12) is about 5% lower than that of J70 and NRLMSIS, and 8% lower than DTM. Since the JB2006 model does not specifically address new geomagnetic formulations, we evaluated it for lower geomagnetic activity conditions. Fig. 5b shows that very similar results are obtained with the data restricted to $ap < 20$. The means/standard deviations for JB2006, J70, NRLMSIS and DTM are respectively 0.98/0.12, 1.02/0.17, 1.00/0.18 and 1.00/0.20. Data for very quiet conditions, $ap < 5$, are shown in Fig. 5c. The means/standard deviations for JB2006, J70, NRLMSIS and DTM are respectively about 0.99/0.13, 1.04/0.18, 0.98/0.17 and 1.00/0.21. Thus the differences in mean values for the various ap bins is within 2% for all models and the standard deviations are essentially constant for each model for these three cases. With the exception of new assimilative modeling techniques²², these results demonstrate that the JB2006 model represents the first significant statistical improvement in thermospheric density specification capability since the inception of the first Jacchia model.

B. Model Accuracy vs Altitude

The scope of the current database allows an unambiguous determination of model errors as a function of perigee altitude. These errors for the JB2006, J70, NRLMSIS and MET models were examined by plotting mean and standard deviation for each individual satellite. While the statistics are determined using the actual satellite altitude, the data for each satellite are plotted at their average perigee altitude. The models are in excellent climatological agreement. Figure 6a shows all mean ratios are within 1 ± 0.05 except for one DTM point at 515 km. The average values over all altitudes are 0.978, 0.996, 1.009, 1.012 and 0.994 for JB2006, NRLMSIS, MET, J70 and DTM respectively. Standard deviations are examined in Fig. 6b. The data show a definite increase in model errors with altitude, as was also demonstrated by Bowman et al¹⁶. As would be expected from the data in Fig. 5, the marked feature of Fig. 6b is that standard deviations for JB2006 are systematically lower than those for the other models at all altitudes. This advantage varies from about 2% (vs J70 and MET) to 6.5% (s DTM) near 218 km to about 6% vs all models near 600 km. The NRLMSIS, J70 and MET model errors all agree closely with altitude. The J70 values fall on those of MET up to about 550 km. Therefore, in agreement with the data of Fig. 5, while all models agree on climatology, the precision of the JB2006 model represents a significant improvement over all other empirical models.

C. Solar Flux Variations

Figure 7a shows differences between the daily values of S_{10} and Mg_{10} indices from F_{10} vs time. (t does not account for the 5-day lag in Mg_{10} used in JB2006). It was also found that the SOHO values were not valid following a drop-out. Therefore these values have been eliminated. The mean differences for $S_{10}-F_{10}$ and $Mg_{10}-F_{10}$ are -0.1 and +2.9 units respectively. The standard deviations are 16 units and 25 units respectively.

It had been previously shown that drag data over 30 years compared to J70 exhibited a non-linear response vs solar flux, with a minimum at solar minimum and a secondary minimum at high solar flux conditions. A fifth-order polynomial provided the best fit to the ratio-flux data distribution. This trend may be due to the inability of F_{10} to represent the density response linearly over the solar cycle²³, or possibly a signature of global cooling²⁴ or some combination and remains under investigation. Density ratios for the present dataset vs solar flux are shown in Fig. 7b. There are large excursions at solar minimum evident in the DTM data. However, again, we were not able to use the MgII option in the model evaluation. Presumably, the chromospheric contributions indicated by Mg II would be more important in this region and provide a better representation in DTM. The model trends are examined as polynomial fits in Fig. 7c. Again, J70 shows the most marked departure from non-linearity with ratios varying from below 0.88 at solar minimum, a maximum of about 1.02 near 120 sfu and a decrease to 0.92 at 225 sfu. This latter value was used due to the lack of high solar flux data points. The DTM values are higher at low flux values as indicated by the data in Fig. 7b. However, it has a sharp drop after reaching a maximum ratio of 1.05 and a value of 0.88 at 225 sfu. The trend is smaller for NRLMSIS with ratios varying from about 0.9 to a maximum of 1.03 and dropping to 0.97 at 225 sfu. For JB2006 data, the trend is almost flat, varying from about 1 at 75 sfu to 0.95 at 250 sfu. The JB2006 ratios vary from 1.01 at solar minimum to 0.94 at 225 sfu. These data tend to suggest that the J70 non-linearities have been reasonably corrected. We were not able to evaluate the contributions of individual solar flux terms in JB2006. Further investigation of the thermosphere response to solar heating is warranted.

The JB2006 model is further compared to NRLMSIS and J70 by examining the data-to-model ratios in latitude-solar flux coordinates. Figure 7d shows ratios, for all 32 satellites combined, in 5 degree latitude and 10 solar flux unit bins. The overall trends vs solar cycle seen in Fig. 7c are again evident. All models perform fairly similarly vs. latitude at a given solar flux value.

D. Day of Year Variations

Figure 8a, from Bowman¹⁸ uses data from selective years to illustrate the capability of JB2006 to represent semiannual (SAV) variations. The amplitude in JB2006 varies with altitude as a function of time, and drops off after an altitude of about 800 km. J70, as well as all previous models, used a climatological average, represented by the pink line. Therefore, a model that can capture features of the previously observed and unmodeled semiannual variation should be expected to reduce model errors. Figure 8b model ratios, shown in latitude-day of year coordinates, demonstrate the fidelity of the JB2006 semiannual formulation. The ratios for JB2006 are generally featureless and the preponderance of ratios are within 1 +/- 0.1. J70 shows, on average, an underestimation of the semiannual variation from December to April and July to September, with data-to-model ratios of up to 1.2, and an overestimation in October-November with ratios as low as 0.8. NRLMSIS also shows the December-April underestimation and a generally less intense overestimation from July-November. DTM highest and lowest ratios are generally at higher latitudes. The high ratios seen to some extent at high northern latitudes around day 182 in all data sets are not explained; no major geomagnetic storms occurred during this period. Thermospheric modeling definitely benefits from the JB2006 semiannual formulation.

E. Local Time Variations

Daily temperature corrections to the J70 model, made as a function of local time, latitude and altitude, were also incorporated into the JB2006 model. Daily temperature corrections to the J70 local time equations were made as a function of latitude, altitude and solar flux based on observations of 114 satellites¹⁶. Model ratios distributed in latitude-local time coordinates are given in Fig. 9 for JB2006, J70, NRLMSIS and DTM. Again, the JB2006 ratios appear to have a generally more limited range than those of J70, NRLMSIS and DTM, indicating the effectiveness of the latest local time corrections. Some of the improved performance may also be due to the reduced semiannual variation errors. NRLMSIS and DTM show diurnal model error trends at low latitudes, with model overestimations near diurnal minimum conditions and underestimations near diurnal maximum conditions. JB2006 shows evidence of an opposite diurnal trend with smaller magnitude. The more pronounced low ratios near 20 hours LT are also evident in the J70 and NRLMSIS models.

F. Geomagnetic Variations

Figure 10 shows model ratios in latitude-daily ap coordinates. The dark stripes in the JB2006 data indicate no data for storms during this period. Generally these storms occur during the period when SOHO data were not available. Very large storms occurred in May, Aug, Sept and Oct 1998. The range of daily ap's from 0 to 40 accounts for 95% of the cases. Over this range all models do reasonably well. For increasingly larger ap values, the Jacchai-based models give the best overall representation of the geomagnetic response. Comparing ap values at zero and 80 units, where, from Fig.4 there are typically only about 5 points per bin, the JB2006 ratios change by only a few percent. NRLMSIS tends to underestimate larger storms on average by about 10-15% and DTM overestimates them by about 15%.

G. Evaluation of JB2006 Model Terms

The improvements in JB2006 over J70 resulting from the new formulations for solar flux, semiannual and diurnal variations were evaluated¹⁶ using satellite data at 400 km. JB2006 was run by removing its semiannual variation formulation and replacing it with that in J70. Standard deviations were reduced from 17.6% for J70 to 13.3% for JB2006 with the J70 SAV formulation. Similarly, it was also found that the new diurnal equations reduced the standard deviation by about 0.5%. The solar flux variation was determined to account for about half of the error reductions achieved by JB2006. Therefore, JB2006 can potentially improve both short term (solar flux) and longer terms (semiannual) variation forecasts.

H. High Altitude Data

High altitude evaluations shown in Fig. 11a use data from the last six satellites in Fig. 1. These satellites are all in polar, near-circular orbits in the altitude region 680-1100 km. We also added data from two satellites between 550-650 km to facilitate comparisons with data in Fig. 6. The mean ratios (top frame) are again close to one for all models except NRLMSIS. The NRLMSIS mean ratios increase from about 6% higher than JB2006 at 680 km to about 25% higher at 1080 km. Picone et al¹⁵ found good agreement between NRLMSIS and J70 data for the combination of summer, high latitude and high altitude (600 to >900 km) data. This comparison was made because the NRLMSIS contains an "anomalous oxygen" during these conditions. Since our evaluation satellites are in near circular orbits, and density is averaged over orbits, it is not possible to extract data in latitude or seasonal bins. The densities used in Fig. 11a were derived using a variable, higher drag coefficient and in JB2006 development. Higher drag coefficients translate into deriving lower densities for a given measured drag. Assuming that the drag coefficient theory used did not apply in this regime, and a value of 2.2 was applicable these densities at 900 km would be increased by an average of about 14%. Further examination is required to evaluate the differences between model density predictions in this altitude regime. Figure 11b shows standard deviations decreasing with altitude, in contrast to the increase below about 600 km shown in Fig. 6b. Again, JB2006 values are lowest, being generally about 5% less than J70 (and MET). Note from Fig. 8a that the SAV amplitude is decreasing above 800 km. The decreased amplitude of the SAV is probably a better representation than the climatological averages in other models.

IV. Summary

An extensive database of satellite drag data has been used to define the performance improvements of the JB2006 model relative to the J70, MET, NRLMSIS and DTM models. The major emphasis was on the altitude region below 600 km where satellite drag has its most important operational impact. The average values (mean ratios of data to model) of model accuracies are similar in this altitude region. However, the standard deviations for JB2006 are lower at all altitudes, by about 4% at 210 km, increasing to about 7% at 550 km. At altitudes above 600 km, JB2006 standard deviations are about 5% lower than those of J70 and MET, and 10% below those of NRLMSIS. Both the improved solar indices and semiannual formulations contribute, approximately equally, to the successful increase in JB2006 model precision. Availability of new EUV direct measurements coupled with a one-day resolution long-term orbital drag database has led to the first (non-assimilative) model to offer a significant advance in neutral density accuracy. The JB2006 is currently the most accurate empirical neutral density model.

Acknowledgments

This effort was supported by the Air Force Space Battlelab under the Sapphire Dragon initiative. We also thank Carolyn Parsons, Boston College for data processing and model inputs, and Neil Grossbard, Boston College for discussions on statistical analyses.

References

- ¹Jacchia, L.G, “Static Diffusion Models of the Upper Atmosphere with Empirical Temperature Profiles”, *SAO Special Report No. 170*, 1964.
- ²Jacchia, L. G. “New Static Models of the Thermosphere and Exosphere with Empirical Temperature Profiles”, *SAO Special Report No. 313*, 1970.
- ³Jacchia, L. G. (1971) “Revised Static Models of the Thermosphere and Exosphere with Empirical Temperature Profiles”, *SAO Special Report No. 332*, 1971.
- ⁴Members of COSPAR Working 4, “*COSPAR International Reference Atmosphere (1972)*”, Akademie-Verlag, Berlin, 1972.
- ⁵Jacchia, L.G., “Thermospheric Temperature, Density, and Composition: New Models”, *SAO Special Report No. 375*, 1977.
- ⁶Owens, J. and Vaughan, W., “Semi-empirical Thermospheric Modeling: The New NASA Marshall Engineering Thermosphere Model - Version 2.0 (MET-V2.0)”, 35th COSPAR Scientific Assembly, 2004, July 2004, Paris, France., p.2708.
- ⁷Barlier, F., Berger, C., Falin, J. L., Kockarts, G., Thullier, G., “A Thermospheric Model Based on Satellite Drag Data” *Annales de Geophysique*, Vol. 34, 1978, p. 451.
- ⁸Berger, C., Biancale, RR., Ill, M., Barlier, F., “Improvement of the Empirical Thermospheric Model, DTM: DTM-94-Comparative Review on Various Temporal Variations and Prospects in Space Geodesy Applications, *Journal of Geodesy*, Vol. 72, 1998, p.161.
- ⁹Bruinsma, S., Thullier, G., and Barlier, F., “The DTM-2000 Empirical Thermosphere Model with New Data Assimilation and Constraints at Lower Boundary: Accuracy and Properties, *Journal of Atmospheric and Solar-Terrestrial Physics*, Vol. 65, 2003, p. 1053.
- ¹⁰Hedin, A. E., Reber, C. A., Newton, G. P., Spencer, N. W., Brinton, H. C., Mayr, H. G., and Potter, W. E., “A Global Thermospheric Model Based on Mass Spectrometer and Incoherent Scatter Data: MSIS 2. Composition”, *J. Geophys. Res.*, Vol. 82, 1977, p. 2148.
- ¹¹Hedin, H.E., Reber, C. A., Spencer, N. W., Brinton, H. C. and Kayser, D. C., "Global Model of Longitude/UT Variations in Thermospheric Composition and Temperature Based on Mass Spectrometer Data", *J. Geophys. Res.*, Vol. 84, 1979 p.1.
- ¹²Hedin, A. E., “A Revised Thermospheric Model Based on Mass Spectrometer and Incoherent Scatter Data: MSIS-83,” *J. Geophys. Res.*, Vol. 88, 1983, p. , 10170.
- ¹³Hedin, A. E., “MSIS-86 Thermospheric Model,” *J. Geophys. Res.*, Vol. 92, 1987, p. 4649.
- ¹⁴Hedin, A. E., “Extension of the MSIS Thermosphere Model into the Middle and Lower Atmosphere,” *J. Geophys. Res.*, Vol. 96, , 1991, p. 1159.
- ¹⁵Picone, J. M., A. E. Hedin, D. P. Drob and Aikin, A. C., “NRLMSISE-90 Empirical Model of the Atmosphere: Statistical Comparisons and Scientific Issues”, *J. Geophys. Res.*, 107(A12), doi 10.1029/2002JA009430. 2002, p. 1468.
- ¹⁶Bowman, B. R., Tobiska, W. K., and Marcos, F. A., “A New Empirical Thermospheric Density Model JB2006 Using New Solar Indices”, AIAA 2006-6166 *AIAA Astrodynamic Conference*, Keystone, CO, Aug. 2006. (Submitted to *J. Geophys. Res.*, 2006).
- ¹⁷Bowman, B.R., and Tobiska, W. K., “Improvements in Modeling Thermospheric Densities Using New EUV and FUV Solar Indices,” AAS 2006-237, *AAS/AIAA Spaceflight Mechanics Meeting*, Tampa, FL, January, 2006.
- ¹⁸Bowman, B.R., “The Semiannual Thermospheric Density Variation From 1970 to 2002 Between 200-1100 km”, AAS 2004-174, *AAS/AIAA Spaceflight Mechanics Meeting*, Maui, HI, 2004.
- ¹⁹Bowman, B. R., Marcos, F. A. and Kendra, M. J., “A Method for Computing Accurate Daily Atmospheric Density Values from Satellite Drag Data”, AAS-04-173, *AAS/AIAA Flight Mechanics Meeting*, Maui, HI, 2004.
- ²⁰Marcos, F. A., “Accuracy of Atmospheric Drag Models at Low Satellite Altitudes”, *Adv. Space Res.*, Vol. 10, (3), 1990, p. 417.
- ²¹Marcos, F.A., Kendra, M. J., Griffin, J., Bass, J. N., Larson, D. R. and Liu, J. J., "Precision Low Earth Orbit Determination Using Atmospheric Density Calibration", *J. Astronaut. Sci.*, 46, 1998, p.395.
- ²²Storz, M. F., B. R. Bowman and Maj. J. L. Branson High Accuracy Satellite Drag Model (HASDM), AIAA 2002-4886, *AAS/AIAA Astrodynamic Specialist Conference*, , Monterey, CA., 2002.
- ²³Marcos, F. A. J. O. Wise, M. J. Kendra, N. J. Grossbard and Bowman, B. R., “Detection of a Long-Term Decrease in Thermospheric Neutral Density”, *Geophys. Res. Lett.*, 32, doi.10.1029/2004GL021269, 2005.
- ²⁴Emmert, J. T., J. M. Picone, J. L. Lean and Knowles, S. H., “Global Change in the Thermosphere: Compelling Evidence of a Secular Decrease in Density”, *J. Geophys. Res.*, Vol. 109, 2004. A02301, doi: 10,1029/2003JA010176., 2004.

Sat No.	Name	Type	B	INCL	Perigee Ht	Apogee Ht	Time
			m ² /kg	Deg	2000 (km)	2000 (km)	
22277	NAV 29 PAM-D	Spheriod	0.02237	34.9	203	9384	1997-2003
6073	VENUS LANDER	Spheriod	0.00356	52.1	213	5431	1997-2003
4053	INTELSAT 3F	Cylinder	0.00582	30.2	264	2828	1997-2003
19824	EXOS D R/B	Cylinder	0.03468	75.0	276	5511	1997-2003
14329	DELTA 1 R/B	Cylinder	0.01892	25.4	280	1200*	1997-1998
14694	WESTAR 6 R/B	Cylinder	0.00196	27.7	289	902	1997-2003
22875	COSMOS 2265	Sphere	0.00807	82.8	300	1243	1997-2002
23853	COSMOS 2332	Sphere	0.00839	82.9	302	1365	1997-2002
8063	DELTA 1 R/B	Cylinder	0.01946	89.2	319	2643	1997-2003
614	HITCH HIKER 1	Octogon	0.01421	82.1	335	2295	1997-2004
2150	OV3-1	Octogon	0.01998	82.4	355	3870	1997-2004
2389	OV3-3	Octogon	0.01796	81.4	356	2968	1997-2004
12388	COSMOS 1263	Sphere	0.01121	83.0	390	1641	1997-2004
60	EXPLORER 8	Dble cone	0.02289	49.9	391	1205	1997-2004
8133	DELTA 1 R/B(1)	Cylinder	0.01956	25.3	394	1215	1997-2004
4221	AZUR (GRS A)	Cone-Cyl	0.02146	102.7	394	2005	1997-2004
7337	COSMOS 660	Sphere	0.01120	83.0	394	1471	1997-2004
8744	COSMOS 807	Sphere	0.01117	82.9	397	1511	1997-2004
23278	COSMOS 2292	Sphere	0.01112	83.0	402	1919	1997-2004
20774	COSMOS 2098	Sphere	0.01138	83.0	403	1852	1997-2004
1616	ATLAS D R/B	Cylinder	0.02016	144.2	404	2510	1997-2004
12138	COSMOS 1238	Sphere	0.01115	83.0	412	1672	1997-2004
14483	COSMOS 1508	Sphere	0.01121	82.9	422	1748	1997-2004
4382	DFH-1 CHINA 1	Spheroid	0.01105	68.4	455	2162	1997-2004
2622	OV1-9 R/B	Cylinder	0.02177	99.1	477	4545	1997-2003
2017	DIAMANT R/B	Cylinder	0.03916	34.1	501	2322	1997-2003
1807	THOR AGENA R/B	Cylinder	0.02550	79.8	505	2738	1997-2003
22	EXPLORER 7	Dble cone	0.02297	50.3	535	844	1997-2003
932	EXPLORER 25	Spheriod	0.02118	81.3	536	2365	1997-2003
11	VANGUARD 2	Sphere	0.05039	32.9	555	3037	1997-2004
47	THOR R/B	Cylinder	0.01970	66.7	599	953	1997-2004
45	TRANSIT 2A	Sphere	0.01615	66.7	605	992	1997-2004
1738	EXPLORER 30	Sphere	0.01572	59.7	681	870	1997-2004
5398	RIGIDSPHERE 2	Sphere	0.06098	87.6	761	849	1997-2004
2909	SURCAL 150B	Sphere	0.19578	70.0	801	817	1997-2004
2826	SURCAL 160	Sphere	0.19279	69.9	812	825	1997-2004
900	CALSPHERE 1	Sphere	0.24239	90.2	999	1061	1997-2004
1520	CALSPHERE 4(A)	Sphere	0.06994	90.1	1083	1189	1997-2004
Total	38					* 1998	

Figure 1. Satellites used in model evaluation, sorted by perigee height. The table provides the satellite number, name, body shape, "true" ballistic coefficient (B), perigee height and apogee height at beginning of year 2000, and overall time period for which data were obtained.

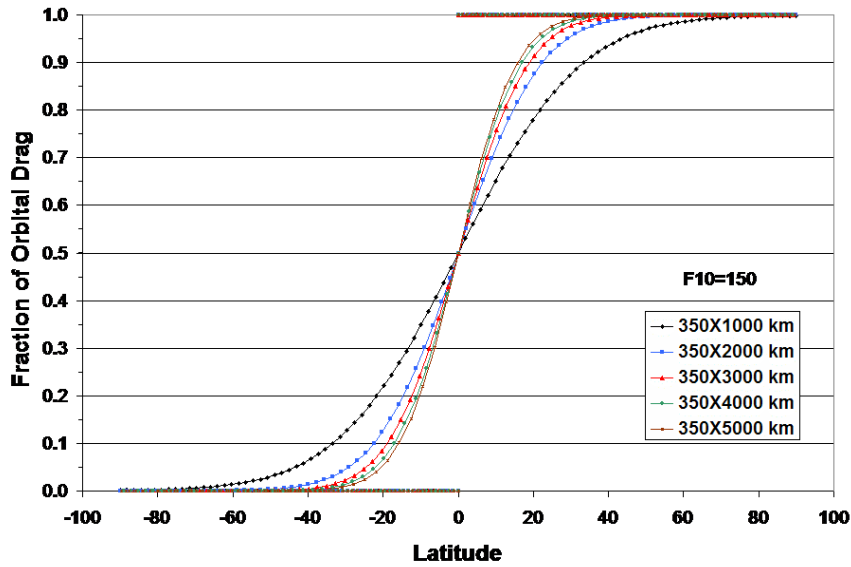


Figure 2. Example of spatial resolution of density values obtained from satellite tracking data

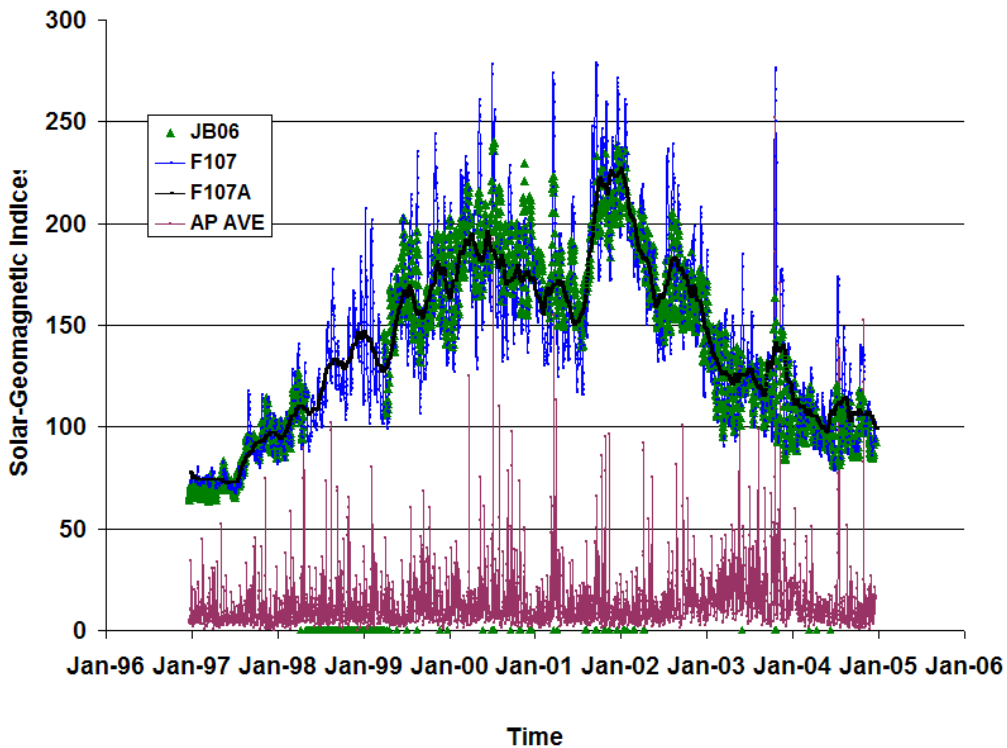


Figure 3. Data availability for JB2006 model and solar and geomagnetic conditions for the period Jan 1997- Dec 2004.

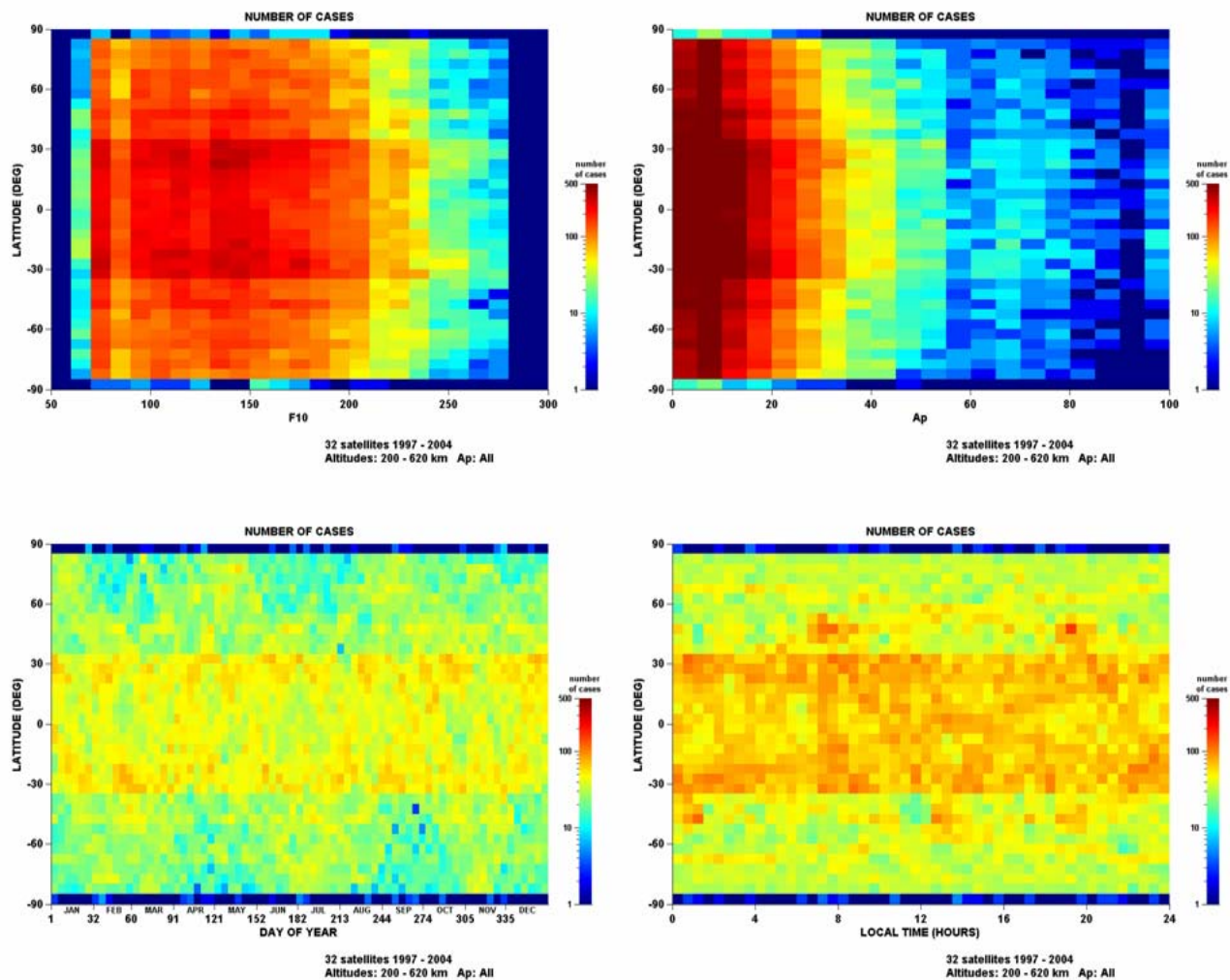


Figure 4. Number of data points vs latitude and (Top left) solar flux, (Top right) geomagnetic activity, (Bottom left) local time and (Bottom right) day of year.

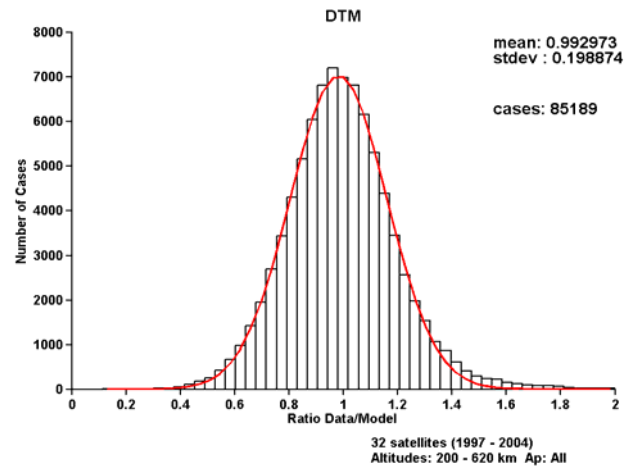
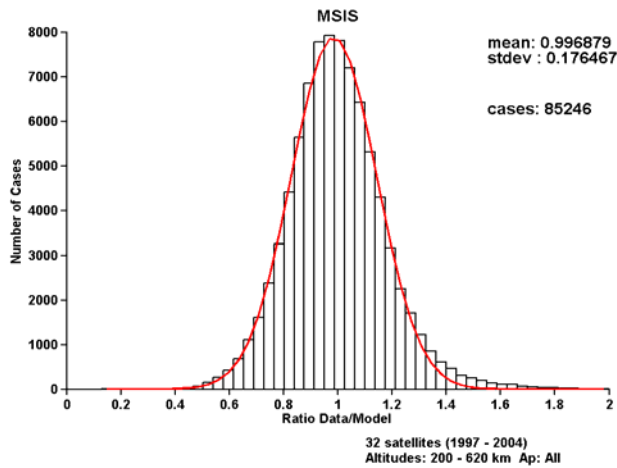
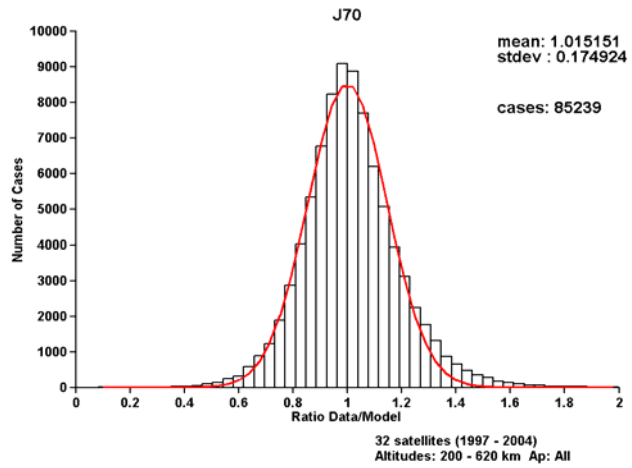
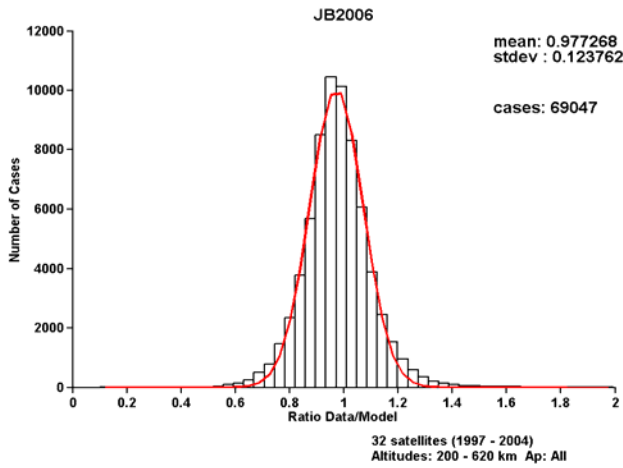


Figure 5a. Frequency distribution of ratios (all ap cases) of orbital drag density data to: (Top left) JB2006 model, (Top right) J70 model, (Bottom left) NRLMSIS model, and (Bottom right) DTM model.

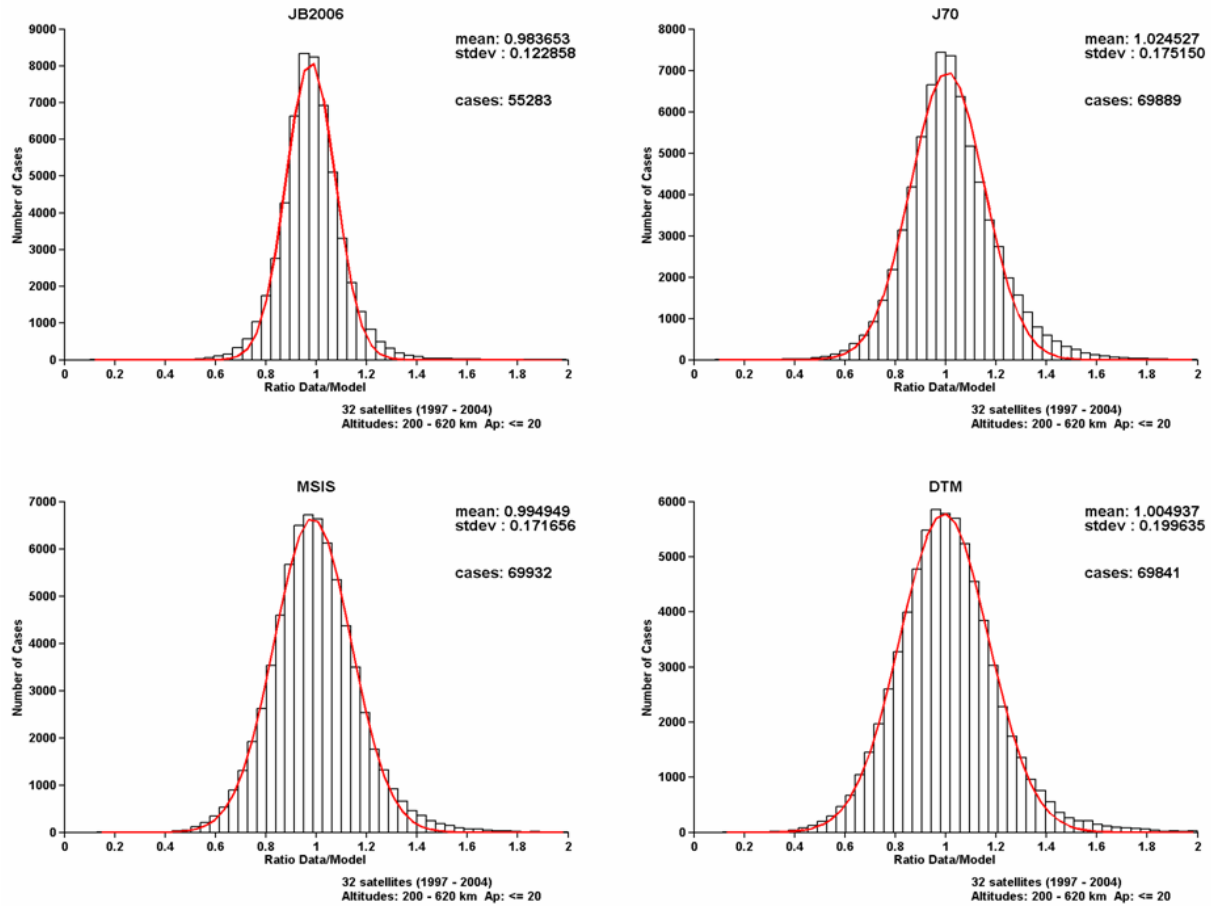


Figure 5b. Frequency distribution of ratios ($ap < 20$ cases) of orbital drag density data to: (Top left) JB2006 model, (Top right) J70 model, (Bottom left) NRLMSIS model, and (Bottom right) DTM model.

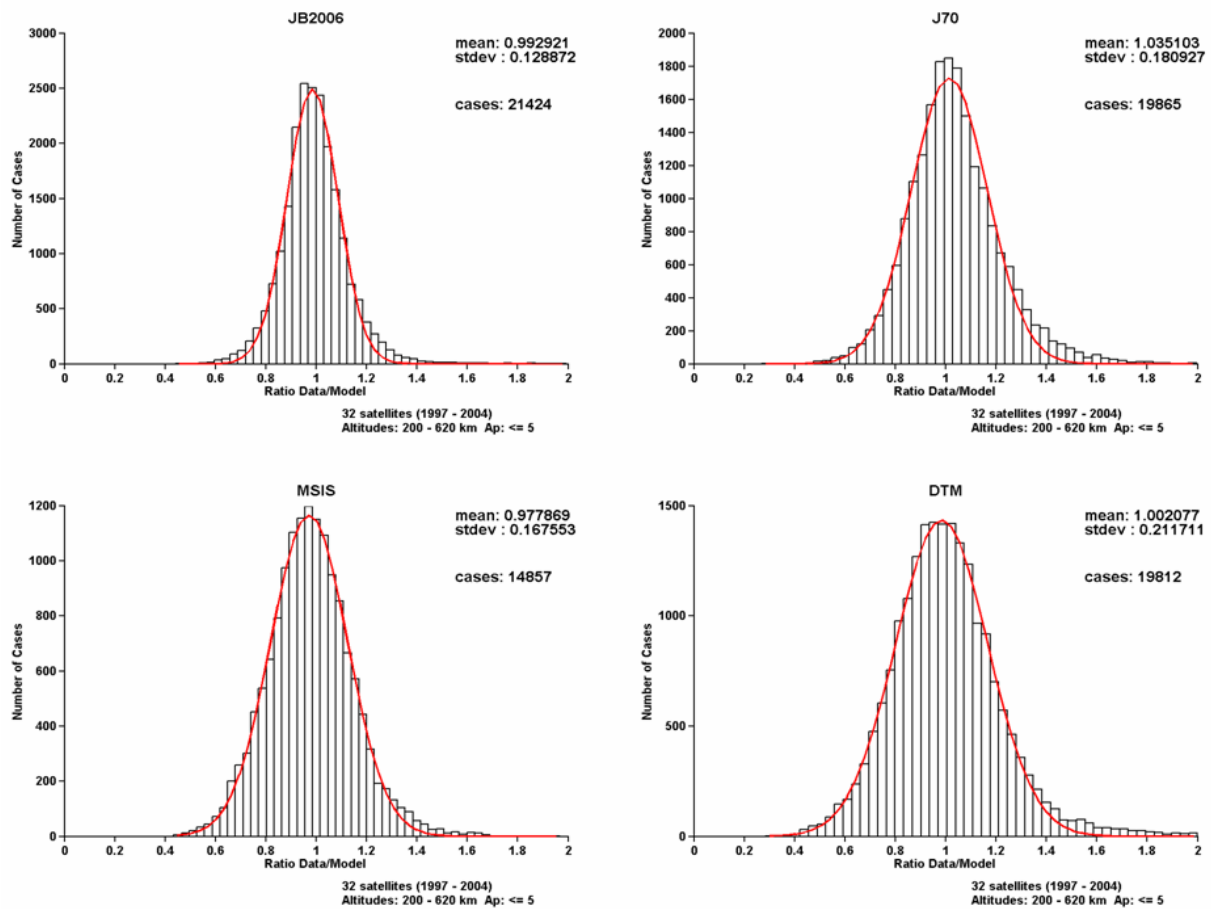


Figure 5c. Frequency distribution of ratios (ap<5 cases) of orbital drag density data to: (Top left) JB2006 model, (Top right) J70 model, (Bottom left) NRLMSIS model, and (Bottom right) DTM model.

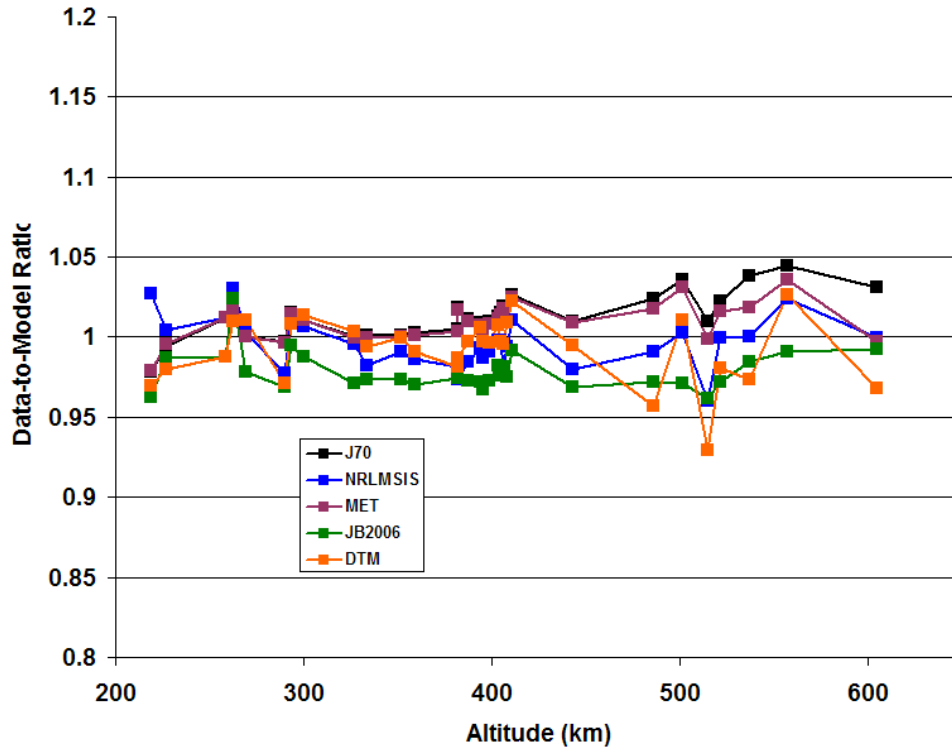


Figure 6a. Mean data-to-model ratios for JB2006, J70, NRLMSIS, MET and DTM models vs altitude.

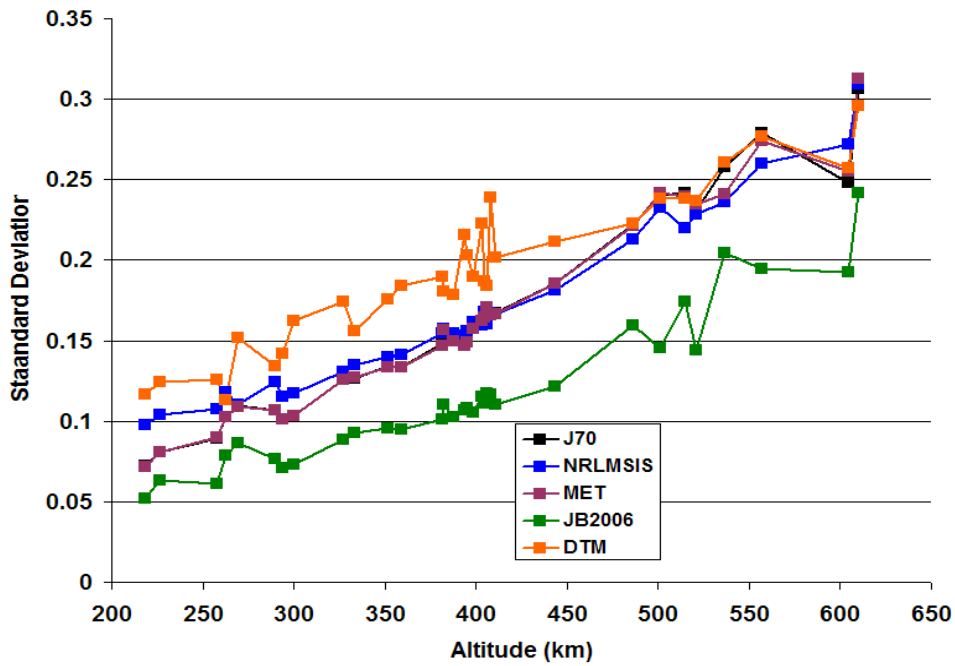


Figure 6b. Standard deviations of data-to-model ratios for JB2006, J70, NRLMSIS, MET and DTM models vs altitude.

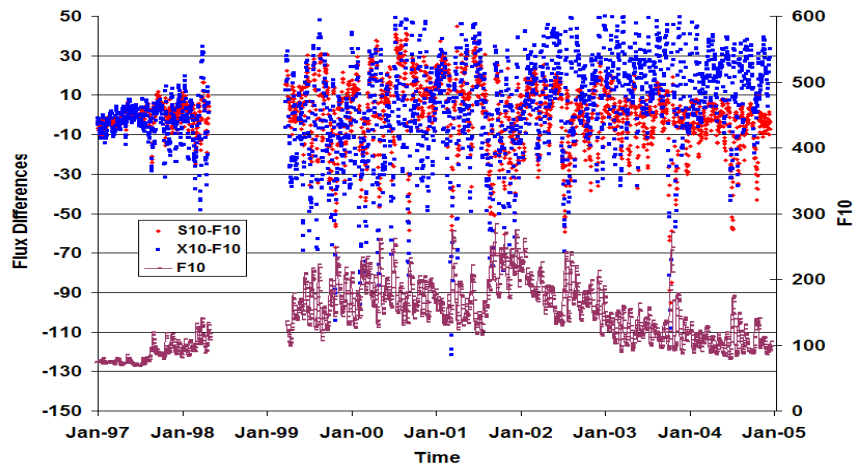


Figure 7a. Differences from F10 for solar indices used in JB2006 model

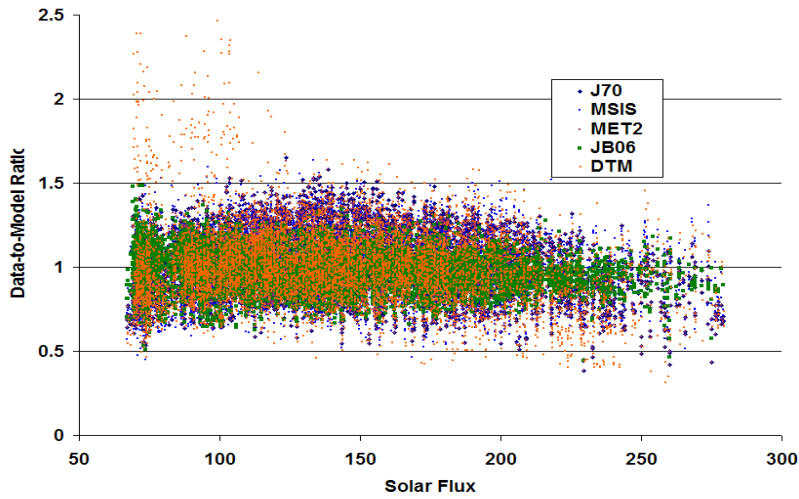


Figure 7b. Data-to-model ratios vs solar flux

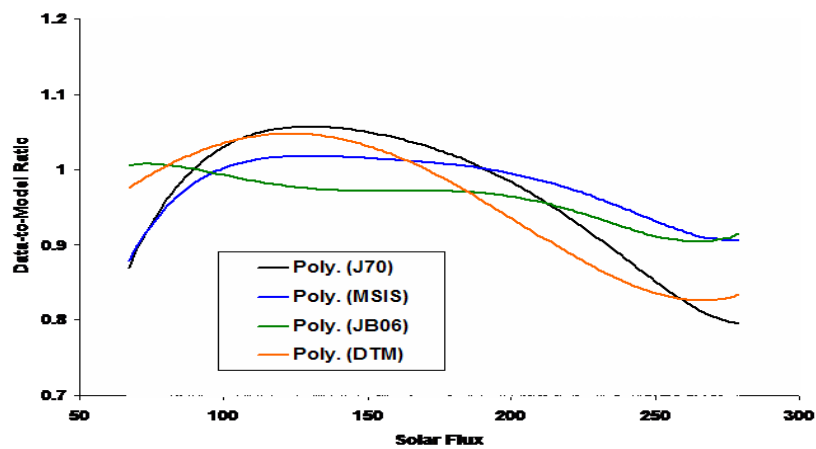


Figure 7c. Polynomial fits to data-to-model ratios.

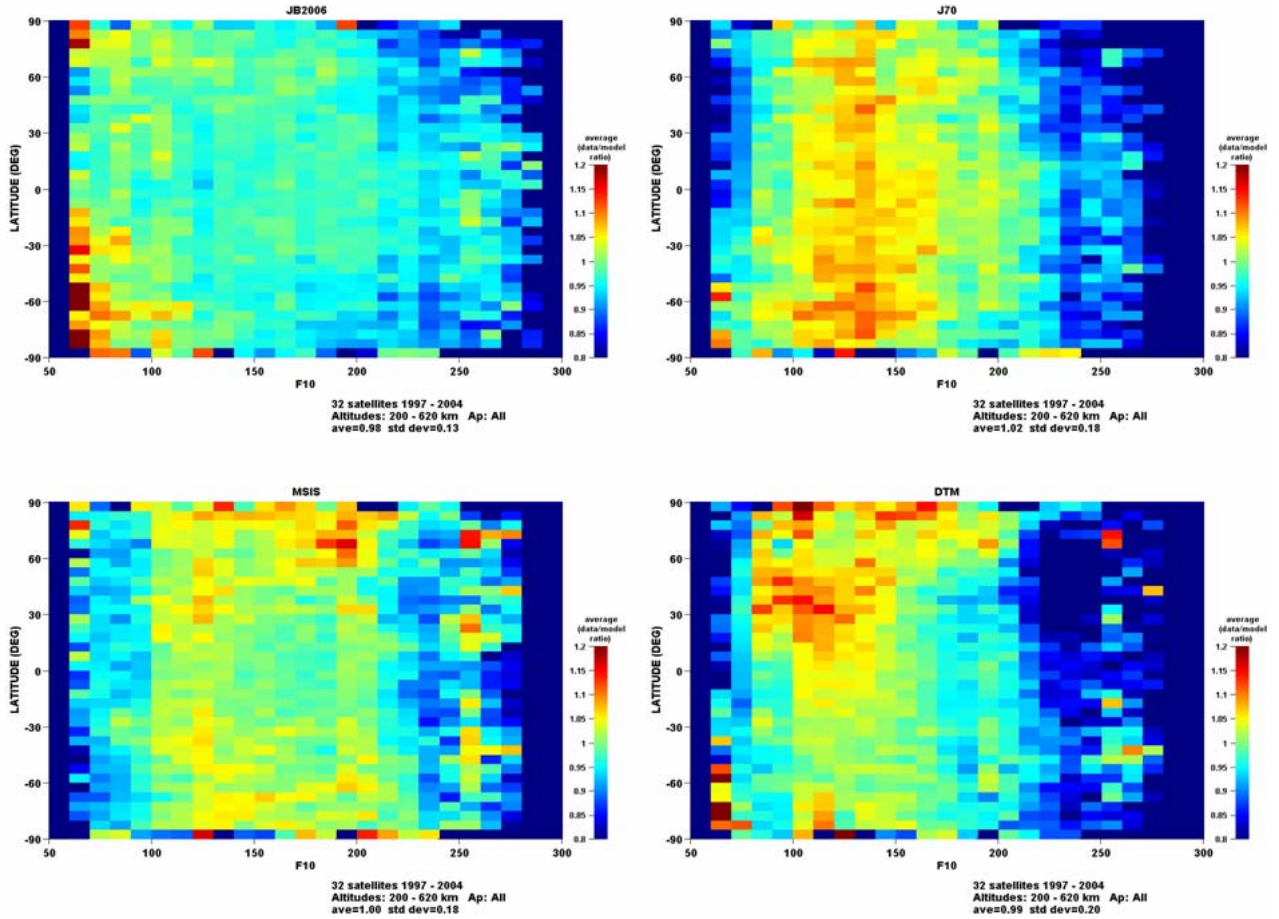


Figure 7d. Data to model ratios in latitude-solar flux coordinates for JB2006 (Top left), J70 (Top right), NRLMSIS (Bottom left), and DTM (Bottom right).

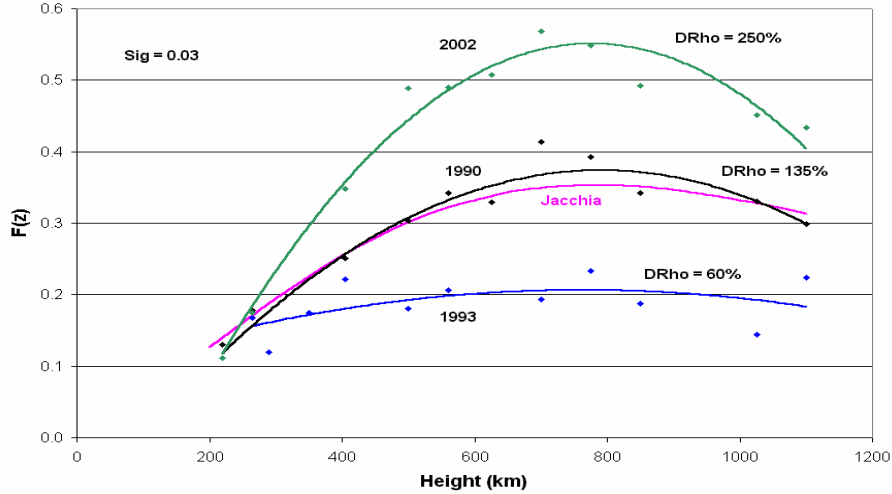


Figure 8a. Example of semiannual variation for different years from JB2006 compared to J70 climatological average.

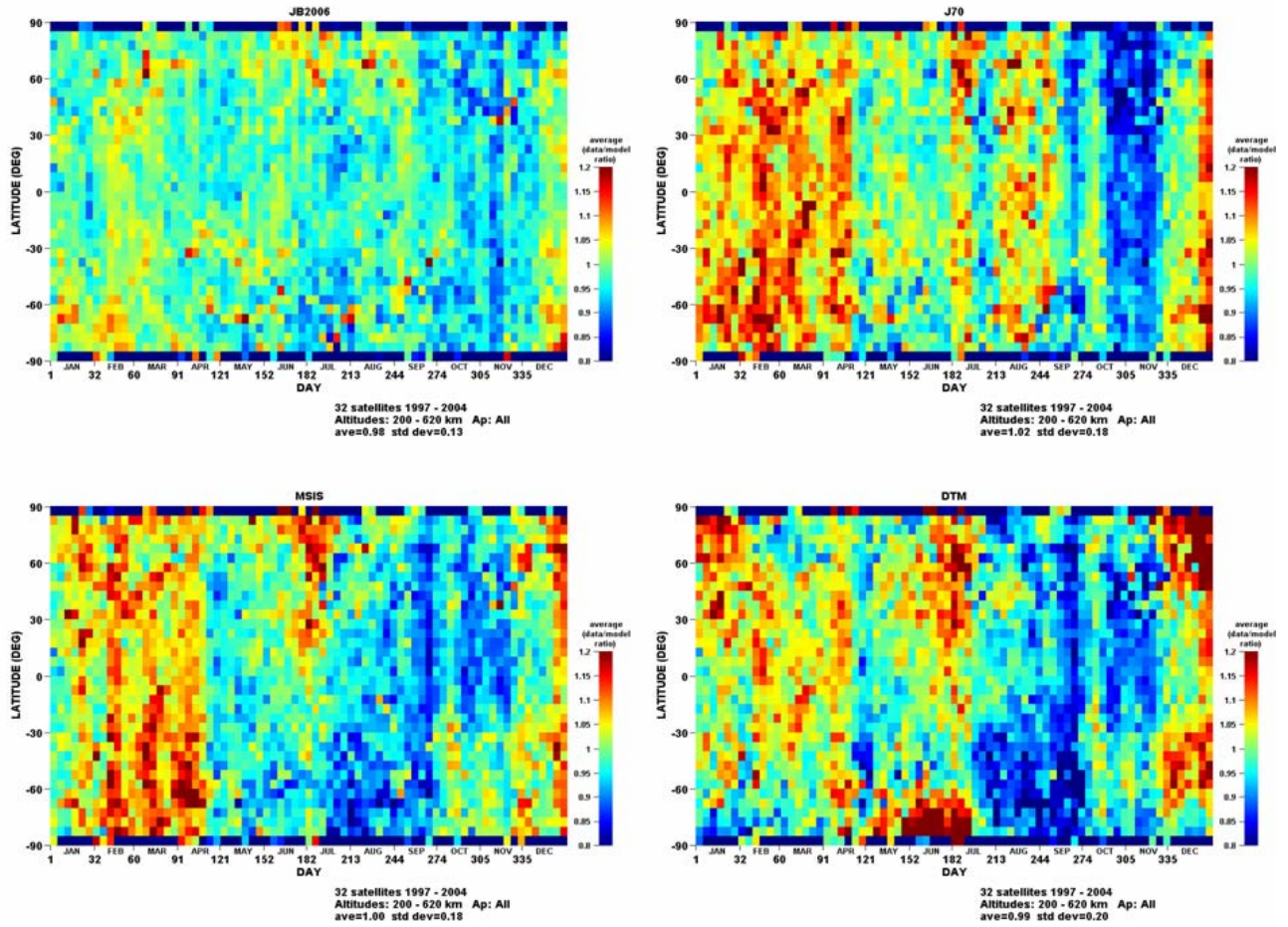


Figure 8b Data-to-model ratios in latitude-day of year coordinates for JB2006 (Top left), J70 (Top right), NRLMSIS (Bottom left), and DTM (Bottom right).

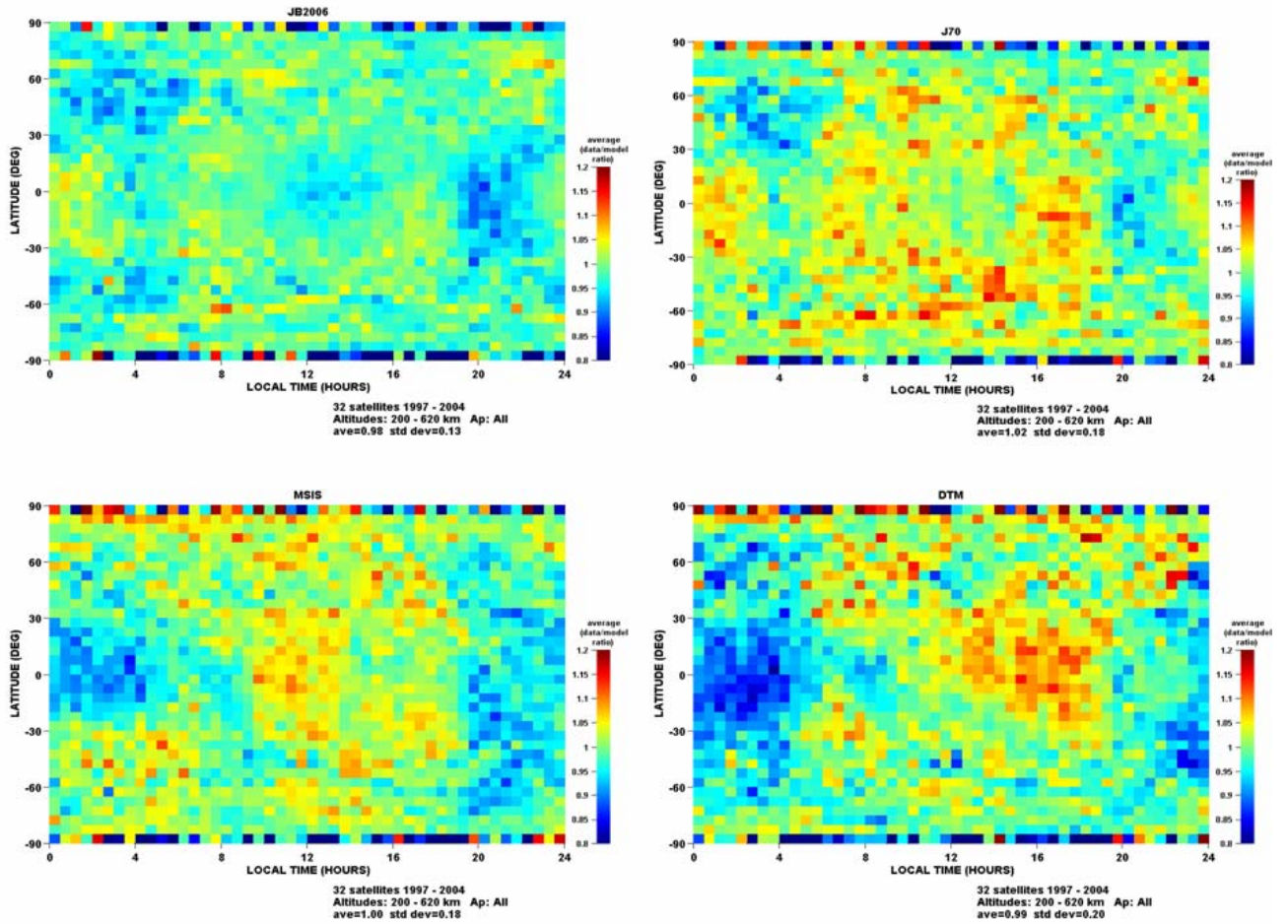


Figure 9. Data to model ratios in latitude-local time coordinates for JB2006 (Top left), J70 (Top right), NRLMSIS (Bottom left), and DTM (Bottom right).

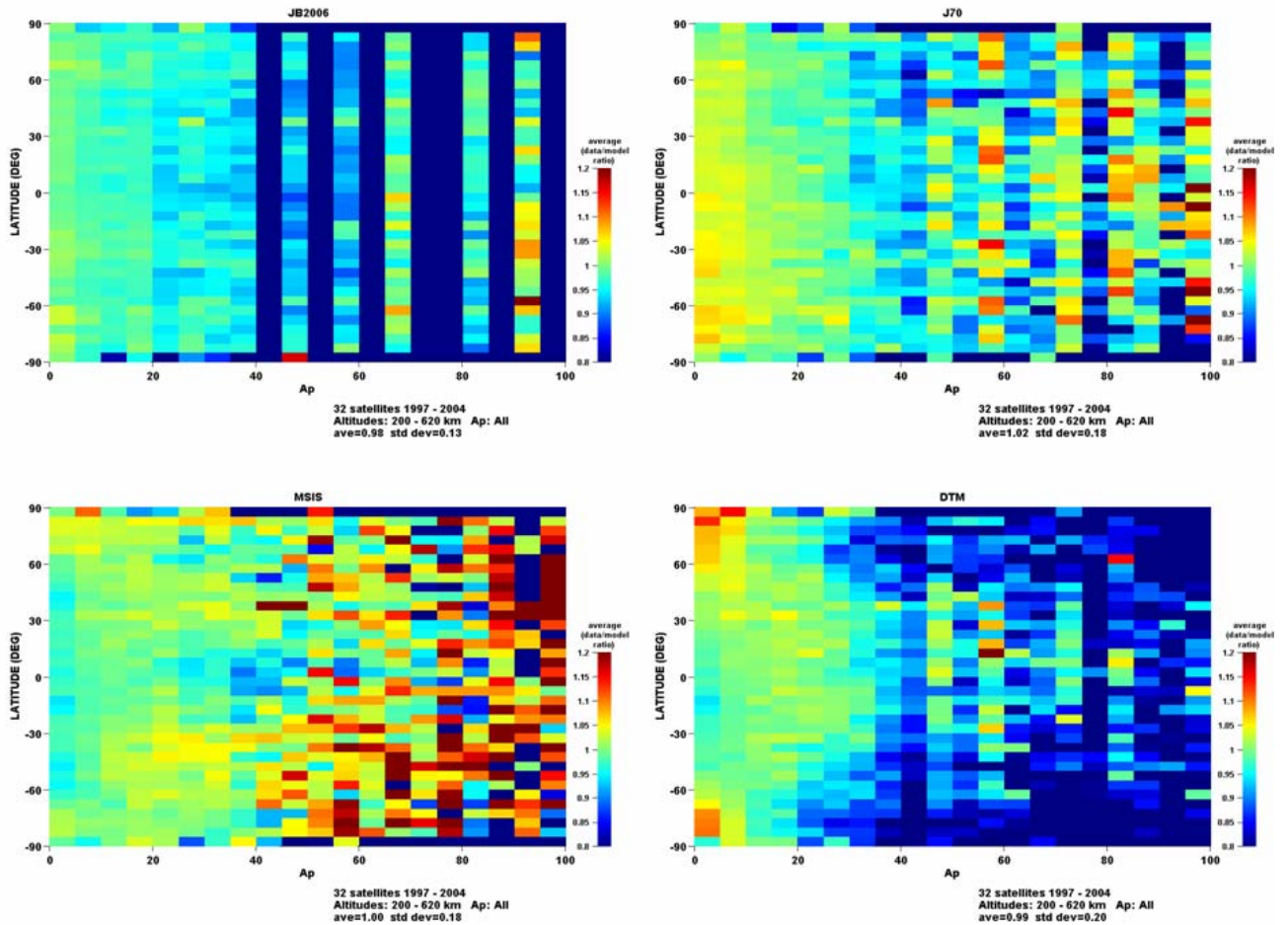


Figure 10. Data-to-model ratios in latitude-geomagnetic activity (ap) coordinates for JB2006 (Top left), J70 (Top right), NRLMSIS (Bottom left), and DTM (Bottom right).

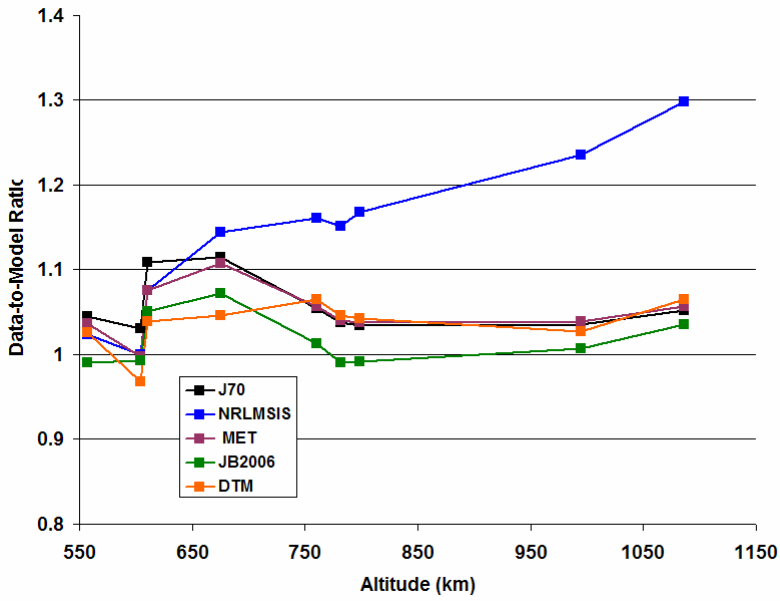


Figure 11a. Mean data-to-model ratios for JB2006, J70, NRLMSIS and DTM models vs high altitude data.

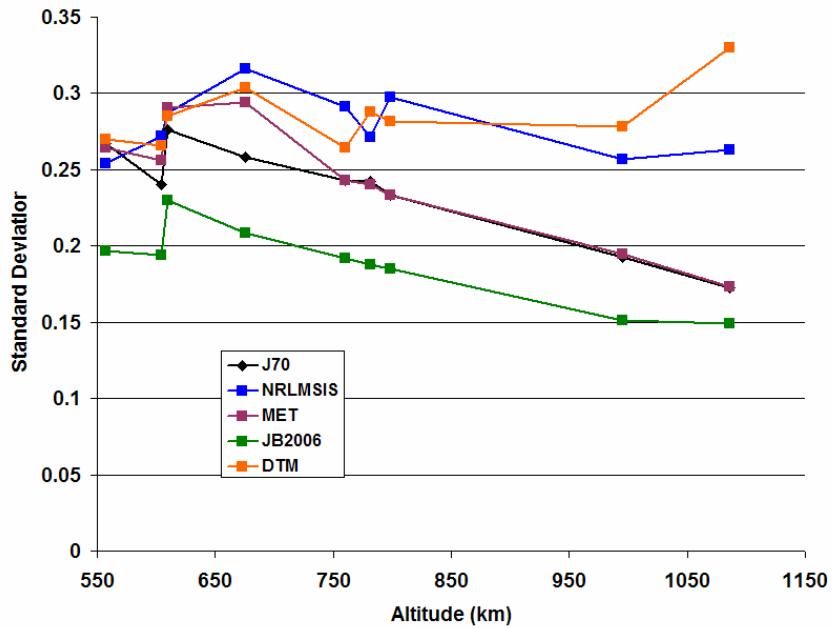


Figure 11b. Standard deviations of data-to-model ratios for JB2006, J70, NRLMSIS and DTM models vs high altitude data.